HUNGARIAN JOURNAL OF
INDUSTRY AND CHEMISTRY
Vol. 53(1) pp. 1–7 (2025)
hjic.mk.uni-pannon.hu
DOI: 10.33927/hjic-2025-01

OXIDIZED MANGOSTEEN PEEL-DERIVED HYDROCHAR FOR THE REMOVAL OF METHYLENE BLUE

SUBODHAN KAMALANATHAN[1], FADINA AMRAN[1] AND MUHAMMAD ABBAS AHMAD ZAINI[1,2]*

1 Faculty of Chemical and Energy Engineering, Universiti Teknologi Malaysia, 81310 UTM Johor Bahru, Johor, MALAYSIA
2 Centre of Lipids Engineering and Applied Research (CLEAR), Ibnu Sina Institute for Scientific and Industrial Research, Universiti Teknologi Malaysia, 81310 UTM Johor Bahru, Johor, MALAYSIA

This work aimed to evaluate the performance of hydrochar and oxidized hydrochars for the removal of methylene blue. Hydrochar was prepared from mangosteen peel, while ammonium persulfate ($(NH_4)_2S_2O_8$), sulfuric acid (H_2SO_4) and nitric acid (HNO_3) were used to oxidize the surface of hydrochars. The performance of pristine hydrochar is better compared to its oxidized counterparts, with a maximum adsorption capacity of 110 mg/g. The adsorption data are well described by Langmuir and pseudo-kinetic models, while the thermodynamic parameters indicate that the process is endothermic and spontaneous. In conclusion, mangosteen peel is a promising feedstock of hydrochar and oxidation treatment may induce a cationic shield that is unfavorable when extracting methylene blue from water.

Keywords: adsorption, hydrochar, mangosteen peel, methylene blue, oxidation treatment

1. Introduction

Although water is essential to sustain all living creatures and for human activities, it is also highly susceptible to pollution [1]. The presence of dyes, heavy metals, microplastics, pesticides, etc. in water jeopardizes the aquatic ecosystem, public health and food chain [2]. The effect of dyes in water has attracted attention because of their complex chemical composition, toxicity and lasting implications for water resources [3]. Even though dyes are usually used to impart color to fabric, paper, etc., the discharge of effluent that is inadequately treated causes water pollution [1].

The methods to treat dye wastewater can be categorized as physical (coagulation and flocculation, adsorption, membrane filtration, etc.), chemical (ozonation, advanced oxidation processes, photocatalysis, etc.) or biological (biosorption, biodegradation, anaerobic digestion, etc.) [4]. The characteristics of contaminants in water and the intended use of the treated water are key factors in determining the most effective treatment strategies. Among others, adsorption is undeniably an effective technique to treat dye wastewater [5]-[6] and is defined as a process whereby the solute is drawn to the solid surface of the adsorbent.

The adsorbent material can be manufactured from various carbonaceous resources such as coconut shells, wood chips, rice husks, fruit peel, etc. This biomass is sustainable, abundant and low-cost [7]. Mangosteen (*Garcinia mangostana*) is a tropical fruit native to Southeast Asia, with a thick outer peel that accounts for approximately 60% of its total mass [8]. The renewable supply of mangosteen peel has sparked interest given its potential as a promising source of biomass for the production of adsorbents.

Adsorbents from biomass can be produced through pyrolysis, surface modification, hydrothermal carbonization, etc. In a related work, hydrothermal carbonization was applied to produce carbon-rich hydrochar from mangosteen peel with a maximum methylene blue capacity of 132 mg/g [9]. In this work, the effect of the surface oxidation of mangosteen peel-derived hydrochar on the removal of methylene blue was studied. Ammonium persulfate ($(NH_4)_2S_2O_8$), sulfuric acid (H_2SO_4) and nitric acid (HNO_3) were used to modify the surface properties of hydrochars. Adsorption took place at different concentrations and temperatures as well as over various contact times in order to investigate the governing removal mechanisms.

2. Experimental

Mangosteen peel was collected from a fruit stall in Johor state, Malaysia before being oven-dried and crushed

Received: 17 June 2024; Revised: 14 Aug 2024;
Accepted: 21 Aug 2024
*Correspondence: abbas@cheme.utm.my

prior to hydrothermal carbonization. $(NH_4)_2S_2O_8$, HNO_3 (65%), H_2SO_4 (98%) and methylene blue (C.I. 52015) of analytical grade were used as received without further purification.

2.1. Preparation and characterization of adsorbents

15 g of dried mangosteen peel was added to 70 mL of distilled water in a Teflon reactor. Hydrothermal carbonization was carried out at 180 °C for 24 h. The resultant hydrochar was oven-dried and the yield calculated to be 75%.

For oxidation treatment, the hydrochar was separately mixed with 50 mL of 0.2 M $(NH_4)_2S_2O_8$, H_2SO_4 and HNO_3 in Beatson Clark bottles before being left in a water bath at 65 °C for 24 h. Next, the resultant oxidized hydrochars were washed with distilled water to remove residual chemicals. All the samples were oven-dried prior to their use. The hydrochar and its oxidized forms (hereinafter referred to as hydrochar adsorbents) were designated as HC (pristine mangosteen peel-derived hydrochar), APS (hydrochar oxidized with $(NH_4)_2S_2O_8$), SA (hydrochar oxidized with (H_2SO_4) and NA (hydrochar oxidized with (HNO_3), respectively.

The thermal degradation profiles of the pristine hydrochar and its oxidized forms were determined using a thermogravimetric analyzer (PerkinElmer, TGA 4000) under a N_2 flow at a heating rate of 10 ºC/min from room temperature to 900 ºC. The surface functional groups were qualitatively identified using a Fourier transform infrared spectrometer (Spectrum One). The surface morphology of the hydrochar adsorbents was obtained by a TM3000 (Hitachi, Japan).

2.2. Adsorption studies

30 mg of hydrochar was added to 30 mL of methylene blue solution of varying concentrations (5-200 mg/L) before being left for 6 days to reach equilibrium. The residual methylene blue (dye) concentration was measured using a visible spectrophotometer and the adsorption capacity at equilibrium, Q_e, calculated as follows:

$$Q_e = \frac{(C_o - C_e)}{m} V \quad (1),$$

where C_o (mg/L) and C_e (mg/L) denote the initial and equilibrium dye concentrations, respectively, V (L) represents the volume of the solution and m (g) refers to the mass of the adsorbent. The adsorption data were analyzed using the Langmuir and Freundlich isotherm models in the following equations, respectively:

$$Q_e = \frac{Q_m b C_e}{1+(bC_e)} \quad (2),$$

$$Q_e = K_F C_e^{1/n} \quad (3),$$

where b (L/mg) denotes the affinity of binding sites, Q_m (mg/g) refers to the maximum adsorption capacity, K_F [(mg/g)(L/mg)$^{1/n}$] represents the relative capacity and $1/n$ stands for the adsorption intensity [10].

The rate of adsorption of the selected hydrochar adsorbents was determined. 30 mg of adsorbent was mixed with 30 mL of dye solution at concentrations of 5, 10 and 20 mg/L. The residual dye concentration was measured at pre-set time intervals until an equilibrium was reached and the capacity at time t, Q_t (mg/g), was calculated as follows:

$$Q_t = \frac{(C_o - C_t)}{m} V \quad (4),$$

where C_t (mg/L) denotes the dye concentration at time t. The kinetic data were analyzed using pseudo-first order and pseudo-second order models as expressed in the following equations, respectively:

$$Q_t = Q_e(1 - e^{-k_1 t}) \quad (5),$$

$$Q_t = \frac{Q_e^2 k_2 t}{1+Q_e k_2 t} \quad (6),$$

where k_1 (min^{-1}) denotes the pseudo-first order rate constant, k_2 (g mg^{-1} min^{-1}) represents the pseudo-second order rate constant and t (min) refers to the contact time.

The thermodynamic parameters were determined from the effect of the temperature on the adsorption of methylene blue. The selected hydrochar adsorbents were mixed with a dye solution at a concentration of 100 mg/L. Adsorption took place at different temperatures, namely 40, 50 and 60 ºC, in a water bath. The parameters of Gibbs energy ($\Delta G°$), enthalpy ($\Delta H°$) and entropy ($\Delta S°$) were calculated using the following equations:

$$\ln(K_d) = -\frac{\Delta H}{RT} + \frac{\Delta S}{R} \quad (7),$$

$$\Delta G = -RT \ln(K_d) \quad (8),$$

$$K_d = \frac{Q_e}{C_e} \quad (9),$$

where K_d denotes the equilibrium constant, while $\Delta H°$ and $\Delta S°$ were calculated from the gradient and intercept, respectively, when $\ln(K_d)$ was plotted against $1/T$.

3. Results and discussion

3.1. Characteristics of the adsorbents

Thermogravimetric analysis (TGA) is an analytical technique that examines variations in the mass of a sample as the temperature increases. The thermal degradation profiles of hydrochar adsorbents are shown in *Figure 1*. The common peaks at 70 °C are ascribed to the release of moisture and light volatiles. The degradation rate increased between 200 and 400 °C, corresponding to the peaks of varying intensities at approximately 300 °C as well as signifying the liberation of thermally sensitive surface functional groups. Their weight gradually decreased at varying rates between 400 and 700 °C, which can be attributed to the fact that HC contains less functional groups as well as indicative of a successful oxidation treatment to produce APS, NA and SA. Furthermore, the presence of thermally-stable

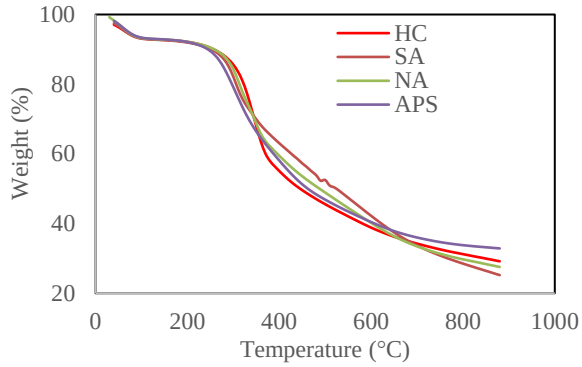

(a)

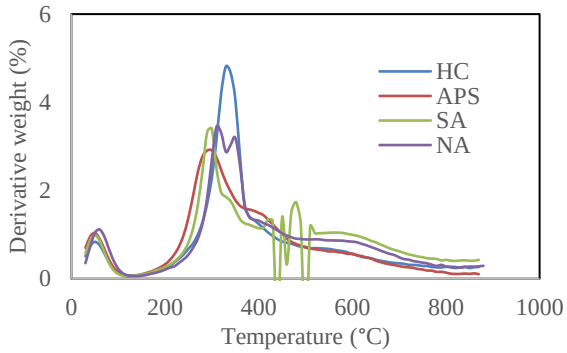

(b)

Figure 1: (a) TGA and (b) DTG profiles of the adsorbents

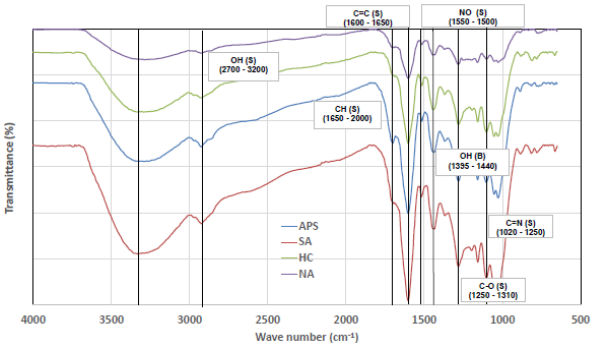

Figure 2: FTIR spectra of the adsorbents

functional groups is implied that act as a protective layer on the hydrochar surface [11].

The weight loss profiles can be characterized by three distinct stages. The initial stage between 5 and 200 ºC coincides with the vaporization of moisture. The second stage between 200 and 600 °C indicates the liberation of volatiles and organic molecules. SA possesses more thermally-stable functional groups than the other hydrochar forms given the steep gradient with some fluctuations during the second stage. Finally, the third stage between 600 and 880 °C is caused by the breakdown of the remaining organic substances [11].

Fourier-transform infrared spectroscopy (FTIR) is a method to determine the chemical makeup of a material. The FTIR spectra of hydrochar adsorbents are shown in *Figure 2*. Functional groups such as hydroxyl (OH),

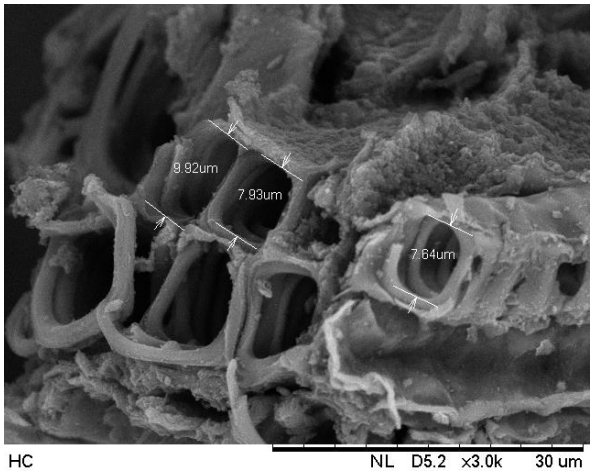

(a)

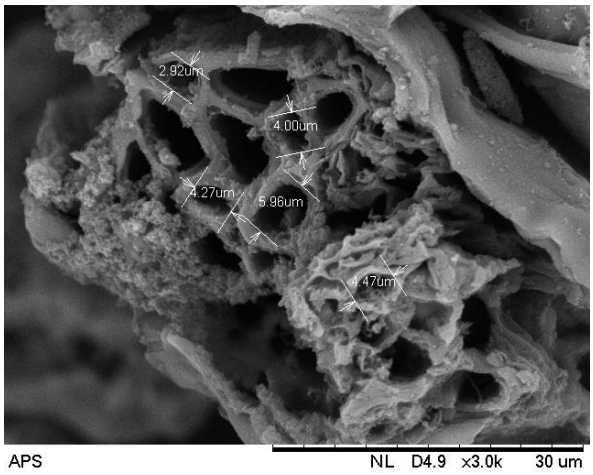

(b)

Figure 3: SEM images of (a) HC and (b) APS

alkane (CH), ether (C=O), nitro (NO), aromatic ester (C–O) and amine (C=N) were identified from the spectra. All hydrochar adsorbents display an abundance of hydroxyl (OH) functional groups, probably due to the inherent/natural moieties in HC and the ones that evolved during the oxidation treatment. HC and NA contain lower concentrations of hydroxyl groups as can be interpreted from the intensity of the peaks.

The SEM images to visualize the surface texture and morphology of the HC and APS are shown in *Figure 3*. The HC surface is more porous compared to that of APS. During hydrothermal carbonization, some functional groups are subjected to thermal decomposition and interact with organic material to produce gases, i.e. carbon monoxide and carbon dioxide, in addition to water vapor [12]. This process alters the morphology and structure of the HC, typically resulting in the specific area expanding. Nevertheless, the porous structure could deteriorate as a result of the substantial loss of material and it collapsing [13].

On the other hand, the oxidation treatment may reduce the number of accessible adsorption sites on hydrochar. The pore opening of HC is larger (8.5 µm) than that of APS (4.3 µm). Notably, oxidation treatment resulted in the pore tunnels of hydrochar shrinking.

Table 1: The constants of isotherm models

Adsorbent	HC	APS	NA	SA
Langmuir				
Q_m (mg/g)	110.0	90.3	74.5	80.8
b (L/mg)	0.39	0.46	0.42	0.32
R^2	0.99	0.96	0.96	0.95
SSE	59	297	219	318
Freundlich				
K_F ((mg/g)(L/mg)$^{1/n}$)	31.0	27.4	22.7	22.9
$1/n$	0.29	0.28	0.27	0.29
R^2	0.91	0.95	0.95	0.97
SSE	819	350	215	163

3.2. Equilibrium adsorption

The adsorption isotherm is essential to determine the surface characteristics and affinity of hydrochar adsorbents towards methylene blue. The equilibrium curves of methylene blue adsorption onto hydrochar adsorbents are displayed in *Figure 4*. Generally, the adsorption of all hydrochar adsorbents increased as the dye concentration increased until their maximum capacities were reached. The high dye concentration is the driving force to encourage the mass transfer of dye molecules to surpass the resistance of the film [14]. The active sites are mostly occupied at high concentrations, ensuring the adsorption capacity remains constant [15].

The constants of isotherm models for the removal of methylene blue by hydrochar adsorbents are shown in *Table 1*. Based on the regression coefficient (R^2) and sum-of-squared errors (SSE), the equilibrium data for HC, APS and NA correspond well with the Langmuir isotherm, while those for SA are better described by the Freundlich isotherm. HC exhibits a greater Q_m of 110 mg/g, followed by APS with 90.3 mg/g, perhaps because of the inherent surface functionalities in the former, while the newly evolved oxygen-containing functional groups in the oxidized forms of hydrochar may enhance steric hindrance (cationic shield), inhibiting the diffusion of dye molecules onto the surface of the adsorbent.

3.3. Adsorption kinetics

Kinetics play a crucial role in the design of a treatment system that relies upon the rate at which pollutants are removed. The rate of dye adsorption onto HC and APS is shown in *Figure 5*. Obviously, their adsorption capacities increased as the contact time increased at all concentrations studied with the adsorption rate of HC being greater than APS. The rate of dye removal varies with contact time due to the transport of dye molecules in order to overcome the boundary layer effect before diffusing into the active sites [16]. Higher concentrations typically require longer contact times to reach

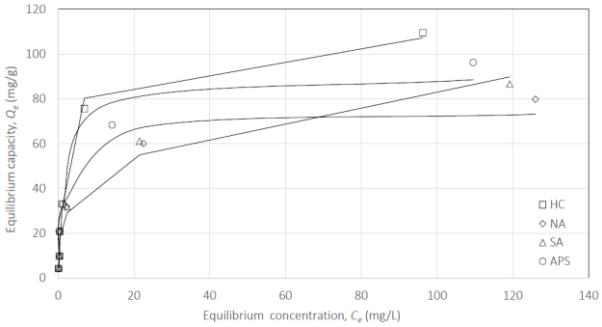

Figure 4: Equilibrium curves of methylene blue adsorption onto hydrochars

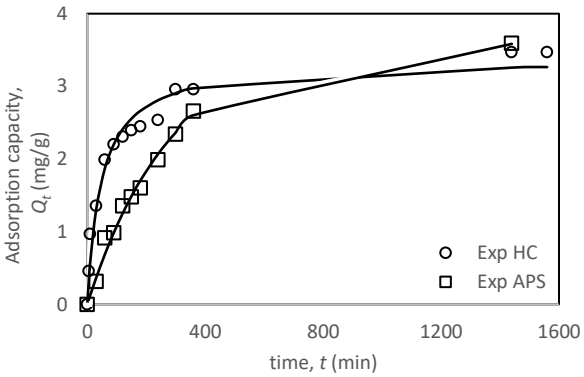

(a)

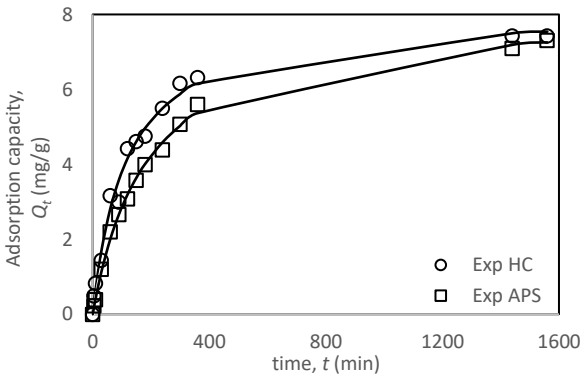

(b)

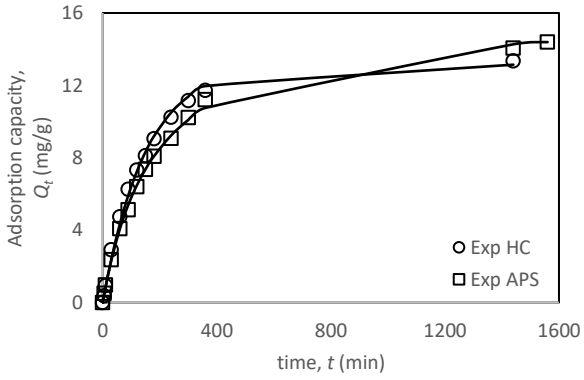

(c)

Figure 5: The rate of methylene blue adsorption by HC and APS at dye concentrations of (a) 5, (b) 10 and (c) 20 mg/L

Table 2: The constants of kinetic models

Adsorbent	HC			APS		
C_o (mg L^{-1})	5	10	20	5	10	20
Pseudo-first order						
Q_e (mg g^{-1})	3.02	7.22	13.10	3.61	7.10	14.00
k_1 (h^{-1})	1.47×10^{-2}	6.77×10^{-3}	6.69×10^{-3}	3.55×10^{-3}	4.59×10^{-3}	4.77×10^{-3}
R^2	0.93	0.99	1.00	0.99	0.99	1.00
SSE	1.31	1.41	0.84	0.12	0.65	1.58
Pseudo-second order						
Q_e (mg g^{-1})	3.37	8.09	14.80	4.37	8.11	16.00
k_2 (g mg^{-1} h^{-1})	6.25×10^{-3}	1.10×10^{-3}	5.83×10^{-4}	8.24×10^{-4}	6.71×10^{-4}	3.55×10^{-4}
R^2	0.97	0.99	1.00	0.99	1.00	1.00
SSE	0.43	0.84	1.09	0.15	0.18	0.40

equilibrium due to several dye molecules competing to attach to the same active site [17]-[20].

From *Table 2*, the kinetic behavior of HC and APS could be described by both pseudo-first order and pseudo-second order models.

The pseudo-first order model describes the rate of adsorption that is directly proportional to the dye concentration, especially when dilute. As the concentration increases, the removal mechanism shifts from physical adsorption to complex interactions between dye molecules and the surface of the adsorbent.

The pseudo-second order rate constant, k_2, decreases as dye concentration increases. As more sites become occupied at higher concentrations, the availability of free sites decreases, thereby decreasing the driving force and adsorption rate. Furthermore, k_2 for APS is slower than that of HC, perhaps due to the evolution of a cationic shield that impedes dye molecules from adsorbing onto the sites.

3.4. Adsorption thermodynamics

The van 't Hoff plot that depicts the adsorption of methylene blue by HC and APS at different temperatures is shown in *Figure 6* and the thermodynamic parameters are summarized in *Table 3*. It is evident that APS consumes more energy (adsorption enthalpy) compared to HC, probably due to the presence of new oxygen functionalities in APS. Since adsorption is endothermic, the dye adsorption capacity increased as the temperature of the solution rose. Raising the temperature of the solution accelerates the movement of dye molecules towards active sites. The negative $\Delta G°$ suggests that the process is spontaneous and favorable, while the positive $\Delta S°$ implies the disorder or randomness of the system during the adsorption process [21].

Table 3: The thermodynamic parameters

Adsorbent	T (K)	$\Delta G°$ (kJ mol^{-1})	$\Delta H°$ (kJ mol^{-1})	$\Delta S°$ (J mol^{-1} K^{-1})
HC	40	-2.86		
	50	-4.68	54.0	182
	60	-6.49		
APS	40	-3.89		
	50	-6.10	65.4	221
	60	-8.32		

3.5. Adsorption mechanisms

The oxidation treatment modifies the surface chemistry of the adsorbent, resulting in the formation of new functional groups, consequently affecting how the different hydrochar adsorbents interact with dye molecules as illustrated in *Figure 7a*.

The presence of oxygen-containing groups in the adsorbent usually facilitates the removal of positively charged pollutants through hydrogen bonding, electrostatic attraction and dispersive interaction [12].

In water, the oxygen-containing functional groups are dissociated, producing a negatively charged surface onto which methylene blue molecules are attracted. However, the excess oxygen functionalities in the oxidized hydrochar inevitably create a H^+ layer covering the surface of the adsorbent as visualized in *Figure 7b*. This protective layer functions as a cationic shield, repelling the cationic dye molecules and hindering their

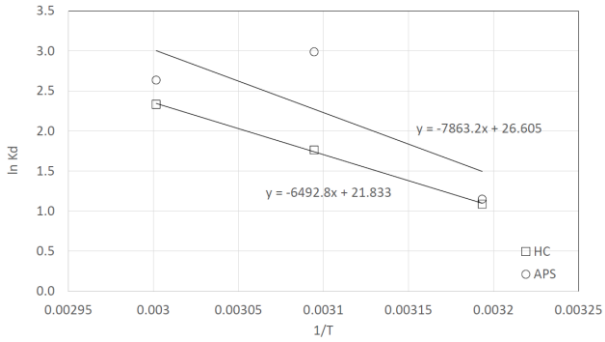

Figure 6: The van 't Hoff plot for methylene blue adsorption onto HC and APS

diffusion to the active sites on its surface. Access to active sites may also be obstructed by water molecules (dipoles) covering the surface. The added oxygen-containing functional groups impede the movement of cations and mass transfer [12]. This combined effect decreases the rate of methylene blue adsorption onto oxidized forms of hydrochar rather than onto the pristine one. In the case of the pristine hydrochar, the dye molecules easily diffuse because of less steric hindrance to occupy its natural functional groups, achieving a greater adsorption capacity.

4. Conclusions

The hydrochar was prepared from mangosteen peel and the oxidation treatment performed using ammonium persulfate, nitric acid and sulfuric acid. The adsorbents were used to remove methylene blue dye in from water. The adsorption behavior, which is endothermic and spontaneous, is well-described by Langmuir isotherm and pseudo-kinetic models with ammonium persulfate-oxidized hydrochar consuming more energy (enthalpy) than its pristine counterpart. The hydrochar prepared from mangosteen peel exhibits a better dye adsorption capacity of 110 mg/g compared to its oxidized counterparts. The oxidation treatment unavoidably induces a cationic shield that impedes the diffusion of dye molecules. Although mangosteen peel is a promising adsorbent feedstock for wastewater treatment applications, more research is needed to unlock the true potential of hydrochar prepared from mangosteen peel.

Acknowledgements

This research was funded by UTM FR No. 23H09.

REFERENCES

[1] Ifguis, O.; Ziat, Y.; Belkhanchi, H.; Ammou, F.; Moutcine, A.; Laghlimi, C.: Adsorption mechanism of Methylene Blue from polluted water by *Opuntia ficus indica* of *Beni Mellal* and *Sidi Bou Othmane* areas: A comparative study, *Chem. Phys. Impact*, 2023, **6,** 100235, DOI: 10.1016/j.chphi.2023.100235

[2] Fan, Z.; Zhang, Z.; Zhang, G.; Qin, L.; Fang, J.; Tao, P.: Phosphoric acid/$FeCl_3$ converting waste mangosteen peels into bio-carbon adsorbents for methylene blue removal, *Int. J. Environ. Sci. Technol.*, 2022, **19**(12), 12315–12328, DOI: 10.1007/s13762-022-03952-z

[3] Jawad, A.H.; Saber, S.E.M.; Abdulhameed, A.S.; Reghioua, A.; ALOthman, Z.A.; Wilson, L.D.: Mesoporous activated carbon from mangosteen (*Garcinia mangostana*) peels by H_3PO_4 assisted microwave: Optimization, characterization, and adsorption mechanism for methylene blue dye removal, *Diam. Relat. Mater.*, 2022, **129**, 109389, DOI: 10.1016/j.diamond.2022.109389

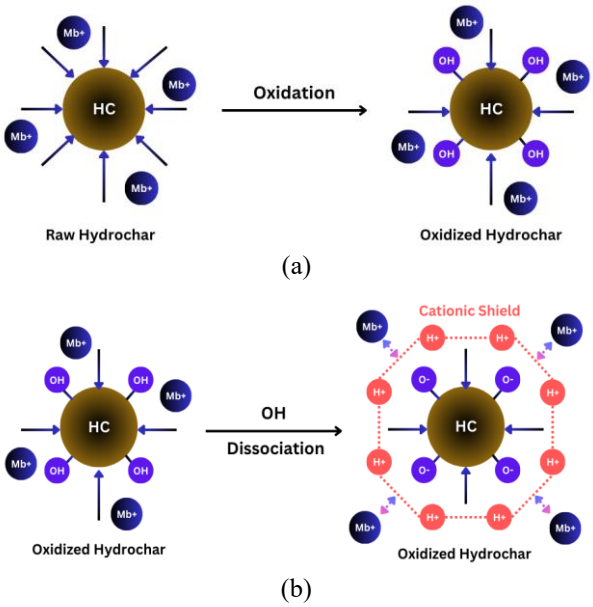

Figure 7: (a) Oxidation of HC and (b) adsorption mechanisms of methylene blue onto oxidized hydrochar

[4] Ghimire, S.; Wang, L.; Zhang, B.; Li, X.; Shahbazi, A.: Production and modification of hydrochar from anaerobically digested cattail for adsorbing ammonium and phosphorous in wastewater, *Water Sci. Technol.*, 2021, **84**(7), 1678–1692, DOI: 10.2166/wst.2021.378

[5] Ramutshatsha-Makhwedzha, D.; Mavhungu, A.; Moropeng, M.L.; Mbaya, R.: Activated carbon derived from waste orange and lemon peels for the adsorption of methyl orange and methylene blue dyes from wastewater, *Heliyon*, 2022, **8**(8), e09930, DOI: 10.1016/j.heliyon.2022.e09930

[6] Nandiyanto, A.B.D.; Fiandini, M.; Fadiah, D.A.; Muktakin, P.A.; Ragadhita, R.; Nugraha, W.C.; Kurniawan, T.; Bilad, M.R.; Yunas, J.; Mahdi Al Obaidi, A.Sh.: Sustainable biochar carbon microparticles based on mangosteen peel as biosorbent for dye removal: Theoretical review, modelling, and adsorption isotherm characteristics, *J. Adv. Res. Fluid Mech. Therm. Sci.*, 2023, **105**(1), 41–58, DOI: 10.37934/arfmts.105.1.4158

[7] Nchoe, O.B.; Sanni, S.O.; Viljoen, E.L.; Pholosi, A.; Pakade, V.E.: Surfactant-modified *Macadamia* nutshell for enhancement of methylene blue dye adsorption from aqueous media, *Case Stud. Chem. Environ. Eng.*, 2023, **8**, 100357, DOI: 10.1016/j.cscee.2023.100357

[8] Samrot, A.V.; Michael, E N.; Anand, D.A.; Mercy, J.L.; Sabesan, G.S.; Mohanty, B.K.; Visvanathan, S.; Saigeetha, S.: The utilization of *Garcinia mangostana* fibers for the removal of crystal violet dye, *Mater. Today Proc.*, 2022, **59**, 1550–1554, DOI: 10.1016/j.matpr.2022.02.232

[9] Hamid, N.A.; You, J.J.: Mangosteen peel-derived hydrochar prepared via hydrothermal carbonization for methylene blue removal, *IOP Conf. Ser.: Earth Environ. Sci.,* 2021, **765**, 012114, DOI: 10.1088/1755-1315/765/1/012114

[10] Tran, T.H.; Le, A.H.; Pham, T.H.; Duong, L.D.; Nguyen, X.C.; Nadda, A.K.; Chang, S.W.; Chung, W.J.; Nguyen, D.D.; Nguyen, D.T.: A sustainable, low-cost carbonaceous hydrochar adsorbent for methylene blue adsorption derived from corncobs, *Environ. Res.*, 2022, **212**, 113178, DOI: 10.1016/j.envres.2022.113178

[11] Madduri, S.; Elsayed, I.; Hassan, E.B.: Novel oxone treated hydrochar for the removal of Pb(II) and methylene blue (MB) dye from aqueous solutions, *Chemosphere*, 2020, **260**, 127683, DOI: 10.1016/j.chemosphere.2020.127683

[12] Qiu, C.; Jiang, L.; Gao, Y.; Sheng, L.: Effects of oxygen-containing functional groups on carbon materials in supercapacitors: A review, *Mater. Des.*, 2023, **230**, 111952, DOI: 10.1016/j.matdes.2023.111952

[13] Blankenship, L.S.; Mokaya, R.: Modulating the porosity of carbons for improved adsorption of hydrogen, carbon dioxide, and methane: a review, *Mater. Adv.*, 2022, **3**(4), 1905–1930, DOI: 10.1039/d1ma00911g

[14] Pathania, D.; Sharma, S.; Singh, P.: Removal of methylene blue by adsorption onto activated carbon developed from *Ficus carica* bast, *Arab. J. Chem.*, 2017, **10,** S1445–S1451, DOI: 10.1016/j.arabjc.2013.04.021

[15] El-Aassar, M.R.; Tamer, T.M.; El-Sayed, M.Y.; Omer, A.M.; Althobaiti, I.O.; Youssef, M.E.; Alolaimi, R.F.; El-Agammy, E.F.; Alruwaili, M.S.; Mohy-Eldin, M.S.: Development of azo dye immobilized poly (glycidyl methacrylate-Co-methyl methacrylate) polymers composites as novel adsorbents for water treatment applications: Methylene blue-polymers composites, *Polymers*, 2022, **14**(21), 4672, DOI: 10.3390/polym14214672

[16] Santhi, T.; Manonmani, S.; Vasantha, V.S.; Chang, Y.T.: A new alternative adsorbent for the removal of cationic dyes from aqueous solution, *Arab. J. Chem.*, 2016, **9**, S466–S474, DOI: 10.1016/j.arabjc.2011.06.004

[17] Yunusa, U.; Usman, B.; Ibrahim, M.B.: Kinetic and thermodynamic studies of malachite green adsorption using activated carbon prepared from desert date seed shell, *Alg. J. Eng. Technol.,* 2020, **20**, 37–45, DOI: 10.5281/zenodo.3659293

[18] Virág, L.; Bocsi, R.; Pethő, D.: Study on adsorption of essential oils on polylactic acid microparticles, *Hung. J. Ind. Chem.*, 2022, **50**(2), 43–49, DOI: 10.33927/hjic-2022-17

[19] Zaini, M.A.A.; Shaid, M.S.M.: Metal chloride-activated empty fruit-bunch carbons for Rhodamine B removal, *Hung. J. Ind. Chem.*, 2016, **44**(2), 129–133, DOI: 10.1515/hjic-2016-0016

[20] Basu, S.; Ghosh, G.; Saha, S.: Adsorption characteristics of phosphoric acid induced activation of bio-carbon: Equilibrium, kinetics, thermodynamics and batch adsorber design, *Process Saf. Environ. Prot.*, 2018, **117**, 125–142, DOI: 10.1016/j.psep.2018.04.015

[21] Zhang, Z.; Xu, L.; Liu, Y.; Feng, R.; Zou, T.; Zhang, Y.; Kang, Y.; Zhou, P.: Efficient removal of methylene blue using the mesoporous activated carbon obtained from mangosteen peel wastes: Kinetic, equilibrium, and thermodynamic studies, *Microporous Mesoporous Mater.*, 2021, **315**, 110904, DOI: 10.1016/j.micromeso.2021.110904